than 1 for any material having a thermal conductivity of order 0.10 Btu/h·ft·°R or greater; thus, most materials of interest would satisfy the assumption of equality of roughness element and smooth wall temperatures. For these cases, there is a net heat transfer from the roughness element to the fluid, because the local static temperature is less than the roughness element's surface temperature over most of the roughness height. If the wall is to be adiabatic, then heat must be transferred from the fluid to the smooth portion of the wall, giving rise to a nonzero temperature gradient at the surface of the smooth portion of the wall.

The authors are unaware of any existing adiabatic wall temperature data on a deterministic rough surface. In order to ascertain the magnitude of the expected change in adiabatic wall temperature due to surface roughness effects, the definition of adiabatic wall temperature described above was implemented in a turbulent, compressible boundary-layer computer program in which surface roughness effects were computed using the discrete element roughness model of Coleman et al.[4] The development and validation of this model are discussed in detail in Refs. 4 and 5. In the discrete element approach the rough surface is assumed to be composed of distinct roughness elements. This model is based on consideration of the physics of the interactions between the discrete roughness elements and the fluid and does not depend on the assumption of any sand-grain equivalent. The physical effects of the roughness elements on the fluid are modeled by considering the flow blockage, the local element/fluid heat transfer, and by postulating that the total force of the elements on the flow can be incorporated as form drag.

The apparent wall shear stress is composed of the viscous shear term acting over the portion of that wall not occupied by roughness elements plus the resultant form drag on the roughness elements. The apparent wall heat transfer is similarly the sum of the heat flux into the smooth portion of the wall plus the net heat diffusion into the roughness elements.

The computer program using the discrete element roughness model was modified to include the option of computing the adiabatic wall temperature over a rough surface. An iterative process was used to determine the surface temperature at which the net heat transfer from the roughness elements was equal in magnitude to the heat transfer to the smooth portion of the wall. This surface temperature is by definition the adiabatic wall temperature of a rough wall.

A study of roughness effects on adiabatic wall temperature was made in which Re_∞/ft, Mach number, roughness height, and roughness spacing ℓ were varied. The Reynolds numbers were $1\text{-}10\times10^6$/ft and freestream Mach numbers of 2.5 and 5.0 were considered. For appropriateness to wind tunnel test conditions, a 5 deg, 2 ft long cone (with the first 1 ft of length smooth) was used as the body shape. Hemispherical roughness elements spaced 3, 4, and 8 radii apart and with radii of 3 and 10 mils were selected as the roughness. These relatively small roughness geometries were chosen in order to ensure that the roughness heights were below the sonic line in the velocity profiles.

Complete results of this study are reported in Ref. 6. Typical results for high and low Reynolds numbers for the $M_\infty = 2.5$ case are presented in Fig. 2. These show that the effect of surface roughness is to reduce the adiabatic wall temperature from the smooth-wall condition. This was something of a surprise since surface roughness typically increases the heat transfer over that for corresponding smooth wall condition. However, the authors feel that this typical increase in *heat transfer* is no basis on which to argue that the *adiabatic wall temperature* for a rough wall should be greater than for the corresponding smooth wall case. As discussed previously, the fluid temperature profile is determined by a local balance of viscous dissipation, convection, and diffusion; and all three of these are influenced by surface roughness.

The results presented herein are consistent within the framework of the roughness model of Coleman et al.[4] and Taylor et al.[5] and serve to demonstrate that surface roughness can alter the adiabatic wall temperature from the smooth-wall value. The results of the study at a Mach number of 5.0 are qualitatively similar to the results at a Mach number of 2.5 and are reported in Ref. 6.

For the high Reynolds number results shown in Fig. 2, the recovery factors are about 0.8, a substantial reduction from the 0.89 predicted by using $Pr^{1/3}$. Burmeister[2] shows smooth-wall recovery factors for air in turbulent flow to be in the range 0.85-0.93 and in laminar flow to be in the range 0.82-0.87. The range of rough-wall turbulent recovery factors found in this study[6] is as large as the range shown by the smooth-wall data for *both* the laminar and turbulent regimes.

Conclusion

The results of the numerical study indicate that surface roughness can have an important effect on adiabatic wall temperature. In particular, surface roughness characteristics, freestream Reynolds number, and freestream Mach number all appear to be important parameters in determining the deviation of the adiabatic wall temperature from the smooth wall value. The results of this study and the absence of experimental data that address the question of surface roughness effects on adiabatic wall temperature indicate a need for additional experimental and analytical work on this problem.

References

[1]Kays, W.M. and Crawford, M.E., *Convective Heat and Mass Transfer,* 2nd ed., McGraw-Hill Book Co., New York, 1980.

[2]Burmeister, L.C., *Convective Heat Transfer,* John Wiley & Sons, New York, 1983.

[3]Cebeci, T. and Bradshaw, P., *Physical and Computational Aspects of Convective Heat Transfer,* Springer-Verlag, New York, 1984.

[4]Coleman, H.W., Hodge, B.K., and Taylor, R.P., "Generalized Roughness Effects on Turbulent Boundary Layer Heat Transfer," AFATL-TR-83-90, Nov. 1983.

[5]Taylor, R.P., Coleman, H.W., and Hodge, B.K., "Prediction of Turbulent Rough-Wall Skin Friction Using a Discrete Element Approach," *Transactions of ASME, Journal of Fluids Engineering*, Vol. 107, June 1985, pp. 251-257.

[6]Hodge, B.K., Taylor, R.P., and Coleman, H.W., "An Investigation of Surface Roughness Effects on Adiabatic Wall Temperature," AIAA Paper 85-1657, July 1985.

Constant-Density Approximation to Taylor-Maccoll Solution

C. S. Moorthy*
Indian Institute of Technology, Kanpur, India

Introduction

THE constant-density solution for steady conical flow in the hypersonic range was studied by several researchers, e.g., Feldman[1] and Hayes and Probstein.[2] In this Note, the Taylor-Maccoll equation is so arranged that the nonlinearities may be grouped into one term which is zero on the cone surface as well as at the oblique shock and that, by neglecting this term, the constant-density approximation may also be used in supersonic range with good accuracy.

Received June 3, 1985; revision received Nov. 25, 1985.

*Professor of Aeronautical Engineering.

The transonic and hypersonic similarity parameters for conical flow may be obtained from those for the wedge flow. At high Mach numbers, a Newtonian approximation can be extracted. For a given half-angle of the wedge or cone, shock detachment occurs at the shock angle at which the density ratio across the shock reaches a maximum value.

Formulation

Let θ, ω, δ_c, and δ be, respectively, the shock angle, polar angle, cone half-angle, and angle of the velocity vector with respect to the cone axis. Let V_r, V_ω, U_1, a, and M be, respectively, the radial, polar, and incident velocities, the speed of sound, and the flow Mach number. The conical steady inviscid irrotational flow equation may be arranged as

$$\frac{d^2V_r}{d\omega^2}+\cot\omega\frac{dV_r}{d\omega}+2V_r=M^2\sin^2(\omega-\delta)\left(\frac{d^2V_r}{d\omega^2}+V_r\right) \quad (1)$$

With ϵ as the ratio of the density ahead of to that behind an oblique shock and δ_s as the flow deflection at the shock, if the equation

$$\left(\frac{d^2V_r}{d\omega^2}\right)+V_r=0 \quad (2)$$

is solved with the conditions that at $\omega=\theta$,

$$V_r=U_1\cos\theta \text{ and } \frac{dV_r}{d\omega}=-\epsilon U_1\sin\theta$$

the solution to Eq. (2) may be written as

$$(1-\epsilon)^{-1}=\sin^2\theta(1+\cot\delta_s\cot\theta) \quad (3)$$

This is exactly the equation obtained from oblique shock relations. Thus, for $(V\omega/a)>1$, the right-hand side of Eq. (1) is zero at the oblique shock as well as on the cone surface where $\omega=\delta=\delta_c$. If the right side of Eq. (1) is assumed to be small between the oblique shock and the cone surface, the result is the Legendre equation. Applying the condition that at $\omega=\delta_c$, $dV_r/d\omega=0$ in addition to those at the oblique shock, the solution to the Legendre equation may be written as

$$(1-\epsilon)^{-1}=\sin^2\theta(1+x\cos\theta) \quad (4)$$

where

$$x=\frac{\cot\delta_c}{\sin\delta_c}+\ell n\left[\frac{\tan(\theta/2)}{\tan(\delta_c/2)}\right] \quad (5)$$

Comparing Eqs. (3) and (4), we obtain

$$\cot\delta_s=x\sin\theta \quad (6)$$

Now, across the oblique shock, $(1-\epsilon)$ may also be expressed in terms of $M_1\sin\theta$, where M_1 is the incident Mach number. Combining this equation with Eq. (4), we may write

$$[\sin^2\theta-(M_1)^{-2}](1+x\cos\theta)=(\gamma+1)/2 \quad (7)$$

where γ is the ratio of specific heats. Using the series expansion of Lees for the velocity components behind the shock and assuming $(\theta-\delta_c)$ to be small, Hammitt and Murthy[3] solved a quadratic valid at high Mach numbers.

The plot of θ vs M_1 for various values of δ_c from Eq. (7) is shown in Fig. 1, along with the exact values taken from Ref. 4. For M_1 between 1.1 and 1.5, the error in θ is less than 10% and, at $M_1=1.75$, it is less than 5%. For given M_1, the error decreases as δ_c increases.

Pressure Coefficient

Using the complete solution to the Legendre equation and Bernoulli's equation for constant density, the pressure coefficient C_p on the cone surface may be written as

$$C_p=(2-\epsilon)\sin^2\theta-(\cos^2\theta/\epsilon)\,[(1-\epsilon)^2(\sin^4\theta/\sin^4\delta_c)-1] \quad (8)$$

Using Eqs. (4) and (7), Eq. (8) may be expressed as

$$C_p=(M_1)^{-2}+(\gamma+3)[2(1+x\cos\theta)]^{-1}-\cos^2\theta$$
$$\times\frac{\{[(\gamma+1)M_1^2/2]+1+x\cos\theta\}}{\{[(\gamma-1)M_1^2/2]+1+x\cos\theta\}}\{[\sin^2\delta_c(1+x\cos\theta)]^{-2}-1\} \quad (9)$$

As $M_1\to\infty$ and $\theta\to\delta_c$, then, $x\cos\theta\to\cot^2\delta_c$. Hence, the first and the last terms on the right-hand side of Eq. (9) tend to zero, so that

$$C_p=[(\gamma+3)/2]\sin^2\delta_c \quad (10)$$

Equation (10) agrees well with the exact values for $\gamma=1.4$ and reduces to Newtonian approximation for $\gamma=1$. For $M_1\sin\delta_c>1$, Eq. (9) may be approximated by

$$\frac{C_p}{\sin^2\delta_c}=\frac{\gamma+3}{4}+\left[\left(\frac{\gamma+3}{4}\right)^2+(M_1^2\sin^2\delta_c)^{-1}\right]^{1/2} \quad (11)$$

The plot of C_p vs M_1 from Eq. (9) is shown in Fig. 2. At Mach numbers below about 1.25, the error is more than 20% for small δ_c and it decreases as δ_c increases. For given δ_c, the error decreases rapidly as M_1 increases.

The plot of $C_p/\sin^2\delta_c$ vs $M_1\sin\delta_c$ from Eq. (11) is shown in Fig. 3. The correlation is good for $M_1\sin\delta_c>1$. The exact points approximately lie between the curve from Eq. (11) and the one obtained from it by replacing M_1^2 by $2M_1^2$ as shown in Fig. 3. The difference between these two curves is similar to that between the small-disturbance approximations of van Dyke and Cole (as compared in Ref. 5) although their correlations are based on $\tan\delta_c$.

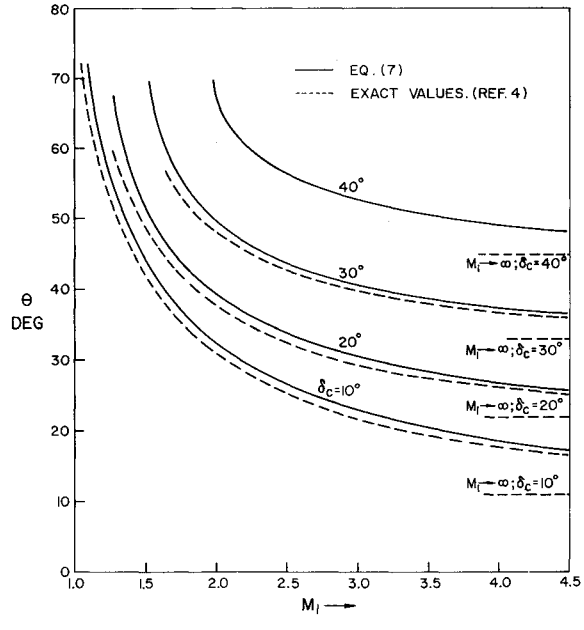

Fig. 1 Shock angle vs Mach number for various cone angles.

Transonic Similarity

In transonic wedge flow, the entropy change depends on the transonic approximation to $(M_1^2\sin^2\theta-1)/(M_1^2-1)$, which leads to the parameter expressed as

$$K_1=(\gamma+1)M_1^2\tan\delta_s/2(M_1^2-1)^{3/2} \tag{12}$$

The transonic parameter for conical flow may be obtained by approximating the right-hand side of Eq. (6) by putting $x=\cot\delta_c/\sin\delta_c$ and θ equal to the Mach angle so that

$$\tan\delta_s=\tan\delta_c(M_1\sin\delta_c) \tag{13}$$

Substituting this equation into Eq. (12) shows that the transonic parameter for conical flow is $M_1\sin\delta_c$ times that for wedge flow of the same half-angle.

Hypersonic Similarity

In hypersonic range, an equation analogous to Eq. (13) may be obtained by approximating for x as in transonic case to find $\sin\theta$ from Eq. (6) and putting $\cos\theta=\cos\delta_c$ in Eq. (4), which then gives

$$\tan\delta_s=(1-\epsilon)^{1/2}\tan\delta_c \tag{14}$$

$$(1-\epsilon)^{1/2}\sin\theta=\sin\delta_c \tag{15}$$

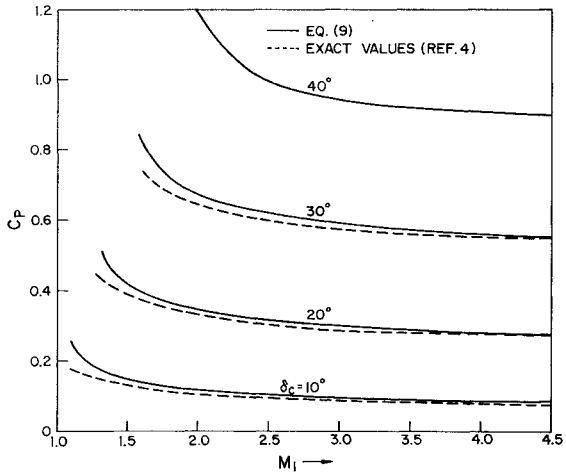

Fig. 2 Surface pressure coefficient vs Mach number for various cone angles.

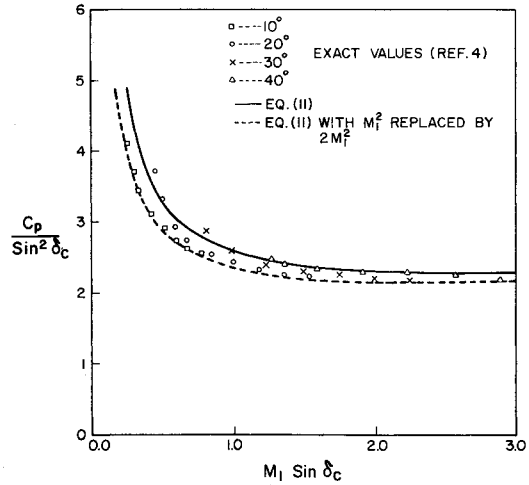

Fig. 3 Similarity for cone surface pressure correlated on the basis of $\sin\delta_c$.

Substituting Eq. (15) into Eq. (8) leads to the same result as Eq. (10) for $\epsilon=(\gamma-1)/(\gamma+1)$. For conical flow, $M_1\sin\delta_c$ may be taken as the hypersonic similarity parameter.

Shock Detachment

For given δ_s, the shock detachment for wedge flow corresponds to $(d\epsilon/d\theta)=0$ in Eq. (3), which gives

$$\theta_d(\text{wedge})=\tan^{-1}(1)+(\delta_s/2) \tag{16}$$

where the subscript d denotes the value at detachment.

A similar result for given δ_c from Eq. (4) gives

$$3\cos\theta(1-3\cos^2\theta)^{-1}=x \tag{17}$$

An approximate expression for θ, whose error is less than 5% for $\delta_c\le 20$ deg and less than 3% for $\delta_c>20$ deg, is

$$\theta_d=\tan^{-1}(2)^{1/2}+(\delta_c/3) \tag{18}$$

Equations (4) and (17) also give

$$\epsilon_d=2\cot^2\theta_d \tag{19}$$

Using Eqs. (6), (17), and (19) at detachment, we obtain

$$(3/\sqrt{2})\epsilon_d^{1/2}\tan\delta_{sd}/(1-\epsilon_d)=1 \tag{20}$$

Using Eq. (14), a shock detachment parameter may be defined in terms of δ_c and ϵ. Substituting Eq. (17) into Eq. (7), the condition on the Mach number for the shock attachment may be expressed as

$$(M_{1d})^{-2}<\gamma+1-[(3\gamma+1)/2]\sin^2\theta_d \tag{21}$$

On the plot of θ vs δ_c for various values of M_1, the detachment line given by Eq. (18) excludes the region of Mach numbers less than M_{1d}. It may, then, be said that the only strong shock possible is the detached normal one. As $M_1\to\infty$, Eq. (21) gives the condition on θ_d,

$$\sin^2\theta_d\le 2(\gamma+1)/(3\gamma+1) \tag{22}$$

For $\gamma=1.4$, the maximum value of θ_d is 73.9 deg and the corresponding value of δ_c from Eq. (18) is 57.6 deg, which agrees well with the exact value of about ~58 deg.

The pressure coefficient at detachment may also be expressed as a function of δ_c.

References

[1]Feldman, S., "Hypersonic Conical Shocks for Dissociated Air in Thermodynamic Equilibrium," *Jet Propulsion*, Vol. 27, 1957, pp. 1253-1255.

[2]Hayes, W. D. and Probstein, R. F., *Hypersonic Flow Theory*, Vol. 1, Academic Press, New York, 1966, pp. 224-227.

[3]Hammitt, A. G. and Murthy, K.R.A., "Approximate Solutions for Supersonic Flow over Wedges and Cones," *Journal of the Aerospace Sciences*, Vol. 27, Jan. 1960, pp. 71-73.

[4]Sims, J., "Tables for Supersonic Flow around Right Circular Cones at Zero Angle of Attack," NASA SP-3004, 1964.

[5]Cole, J. D., "Newtonian Flow Theory for Slender Bodies," *Journal of the Aeronautical Sciences*, Vol. 24, June 1957, pp. 448-455.